Solar-Terrestrial Physics. 2025, vol. 11, iss. 2, pp. 69–77. DOI: 10.12737/stp-112202507. © 2025 K.G. Ratovsky, M.V. Klimenko, A.M. Vesnin, K.V. Belyuchenko. Published by INFRA-M Academic Publishing House

DOI: 10.12737/stp-112202507

Received October 02, 2024
Accepted April 02, 2025

REGIONAL ELECTRON CONTENT RESPONSES TO GEOMAGNETIC EVENTS AT HIGH, MIDDLE, AND EQUATORIAL LATITUDES OBTAINED BY SUPERPOSED EPOCH METHOD USING *AE* INDEX

K.G. Ratovsky
Institute of Solar-Terrestrial Physics SB RAS, Irkutsk, Russia, ratovsky@iszf.irk.ru

M.V. Klimenko
West Department of Pushkov Institute of Terrestrial Magnetism, Ionosphere and Radio Wave Propagation RAS, Kaliningrad, Russia, maksim.klimenko@mail.ru

A.M. Vesnin
Institute of Solar-Terrestrial Physics SB RAS, Irkutsk, Russia, artem_vesnin@iszf.irk.ru

K.V. Belyuchenko
Institute of Solar-Terrestrial Physics SB RAS, Irkutsk, Russia, kdei@list.ru

Abstract. The paper studies statistical patterns of regional electron content responses to geomagnetic events at high, middle, and equatorial latitudes. The regional electron content is the total electron content averaged over all longitudes in a given latitudinal zone. The statistical analysis includes the following: 1) identification of geomagnetic events based on the *AE* index and calculation of "reference" geomagnetic storms; 2) calculation of the regional electron content (*REC*) for five latitudinal zones (equatorial zone, mid-latitude zones of the Northern and Southern hemispheres, and high-latitude zones of the Northern and Southern hemispheres); 3) calculation of *REC* disturbances (Δ*REC*), which are relative (percentage) deviations of the observed values, from the 27-day running mean of *REC* and 4) obtaining the "reference" ionospheric response in the form of the dynamics of average Δ*REC*, obtained by the superposed epoch method. The superposed epoch method is implemented with the hourly resolution and key moments corresponding to the *AE* index maximum. Compared with our previous statistical analysis, implemented with daily resolution based on geomagnetic storm identification by the *Dst* index, the new method leads to a significant increase in the amplitude and the time-focusing of the response. The seasonal behavior of ionospheric responses was analyzed for correspondence to the thermospheric storm concept. The responses of the equatorial and mid-latitude zones of the Southern Hemisphere fit the thermospheric storm concept. In the mid-latitude zone of the Northern Hemisphere, there are a number of exceptions. The responses of the high-latitude zone show the need to take into account the mechanisms behind the formation of positive disturbances, which are absent in the thermospheric storm concept.

Keywords: ionospheric response, geomagnetic storm, statistics, superposed epoch method, *AE* index.

INTRODUCTION

Solar, geomagnetic, and meteorological activity contribute to the general ionospheric variability. Statistical analysis of ionospheric variability has shown that the contribution of meteorological and geomagnetic activity is estimated approximately equally: 13–15 % of all disturbances of the peak electron density N_mF2 for the dayside mid-latitude ionosphere [Araujo-Pradere et al., 2005; Rishbeth, Mendillo, 2001; Deminov et al., 2011]. Statistical analysis of ionospheric responses to geomagnetic storms [Ratovsky et al., 2018] has revealed that even in the case of isolated storms occurring in the same seasons at roughly the same time of day ionospheric responses can differ considerably from each other. A reason for such differences can be ionospheric disturbances of meteorological origin, which have sources in the lower atmosphere, as well as uniqueness of each geomagnetic storm. Simulation results [Pedatella, 2016; Pedatella, Liu, 2018; Klimenko et al., 2023] have demonstrated that it is important to take into account atmospheric conditions when analyzing the ionospheric response to geomagnetic storms. These facts greatly complicate the problem of forecasting space (including ionospheric) weather during geomagnetic storms.

Ionospheric responses to geomagnetic events can be studied by two approaches. The first approach is to examine the response to a specific geomagnetic storm or a set of a small number of storms. The second (statistical) approach is aimed at obtaining an ionospheric response averaged over an ensemble of similar storms (within some selected criteria). It is expected that the second approach has the advantage that the averaged ionospheric response will generally depend on effects of the magnetic storm per se, whereas the effect of processes in the lower atmosphere will be reduced by averaging. As previous studies have shown [Ratovsky et al., 2020], isolated storms occur in different phases of 27-day variations in solar activity, which reduces the effect of these variations on the ionospheric response by averaging over an ensemble of isolated storms.

For the first time, the statistical approach was proposed in [Wrenn et al., 1987], where ionospheric responses were sorted into cells according to local time, month of the year, and geomagnetic activity level, determined by the integral index A_p to obtain the average steady state disturbance. This approach was developed when constructing an average diurnal-seasonal pattern of the mid-latitude N_mF2 response [Rodger et al., 1989] and when analyzing the interhemispheric asymmetry of total electron content (*TEC)* disturbances [Titheridge, Buonsanto, 1988].

In previous studies, we have proposed a statistical approach to obtaining a pattern of average response to geomagnetic storms for the following ionospheric characteristics: daily average N_mF2 at Irkutsk and Kaliningrad [Ratovsky et al., 2018] and daily average *REC* for five latitudinal zones [Ratovsky et al., 2020]. In all cases: the time resolution was 1 day; geomagnetic storms were identified by *Dst*; the average ionospheric response was calculated by the superposed epoch method with a key date corresponding to the day of minimum *Dst* in UT.

A disadvantage in using diurnal resolution is that the ionospheric response at a key date is a mixture of pre-storm disturbances, response effects during the magnetic storm main phase and early recovery phase. With minimum *Dst* near 0 UT, it is a response to the recovery phase; with minimum *Dst* near 23 UT, a response to the main phase in combination with pre-storm disturbances; in other cases, the response is intermediate. This shortcoming prompted us to employ the hourly resolution in the future. Another feature of the proposed approach is the use of *Dst* as an indicator of a geomagnetic event. The advantage of *Dst* is that the concept of magnetic storm main and recovery phases has been developed for this index, as well as the identification and classification of magnetic storms according to minimum *Dst* [Gonzaleze et al., 1994, 1999]. At the same time, the geomagnetic event indicator, which is most closely related to the ionospheric response, is useful for ionospheric research. According to the analysis carried out in [Prölss, 2006; Lu et al., 2001], such an indicator is the *AE* index. It is this index that shows a high correlation with the Joule heating of the high-latitude and auroral ionosphere during geomagnetic storms [Prölss, 2006; Lu et al., 2001], which, in turn, is one of the main causes of ionospheric disturbances according to the thermospheric storm concept. An added incentive is that *AE* is one of the control parameters for physical models of the ionosphere such as GSM TIP [Klimenko et al., 2011]. Statistical studies have shown that High-Intensity Long-Duration and Continuous *AE* Activity (HILDCAA) generates significant *TEC* disturbances at low latitudes [da Silva et al., 2020]. These considerations led us to use *AE* as an identifier for geomagnetic events. The nuances associated with replacing *Dst* with *AE* are discussed in the next section.

Thus, the paper presents a modification of the previously proposed statistical approach to studying ionospheric responses to geomagnetic storms [Ratovsky et al., 2018; Ratovsky et al., 2020], based on the use of hourly resolution instead of diurnal and *AE* instead of *Dst*. Results of this modification are discussed in the corresponding section. Note that these indices describe completely different current systems despite being indicators of geomagnetic activity. Thus, *AE* measures variations in auroral currents; and *Dst*, in ring currents.

DATA ANALYSIS METHOD

In this work, we employ geomagnetic activity indices and global ionospheric maps of *TEC* for 1999–2018. The choice of 1999 is due to the fact that this year is the first year of complete global *TEC* maps; the choice of 2018, the *AE* values in the database we use [https://omniweb.gsfc.nasa.gov] are available only until 2018. Further analysis is based on hourly average *AE*.

The *AE*-based method of identifying geomagnetic events is detailed in [Ratovsky et al., 2024]. It is similar to the previously developed method of identifying geomagnetic storms by *Dst*, except that instead of minimum *Dst* we employ maximum *AE*, and the *AE* threshold value for event identification should provide the number of geomagnetic events closest to the number of storms obtained under the *Dst* criterion with threshold *Dst*=–50 nT. Ratovsky et al. [2024] provide the following justifications for the selected method of determining threshold values. The threshold level of the K_p index, obtained by the same method as for *AE*, yields K_p=5, which is fully consistent with the threshold for a geomagnetic storm under the K_p criterion according to NOAA Space Weather Scales. The threshold value of *AE*=930 nT is close to *AE*=1000 nT used in [Marques de Souza Franco et al., 2021] for identifying HILDCAA events. In most cases, geomagnetic events identified by *AE* correspond to geomagnetic storms according to the *Dst* criterion. As a result, the criterion for a geomagnetic event identified by *AE* was the fulfillment of two conditions: 1) $AE(t_0)$ is the highest *AE* for the time interval t_0±12 hrs; 2) $AE(t_0)\geq$930 nT, where t_0 is the time corresponding to maximum *AE*. We have identified 554 geomagnetic storms according to the *Dst* criterion and 556 geomagnetic events according to the *AE* criterion. Comparing the lists of identified events has shown that geomagnetic events according to the *AE* criterion in 469 of 556 cases (i.e. in 84 % of cases) occur during geomagnetic storms according to the *Dst* criterion. Thus, by the *AE* criterion, in most cases the event is a magnetic storm; in the remaining cases it is an intense substorm under undisturbed conditions. In what follows, geomagnetic events identified by *AE* are referred to as *AE* storms.

As previous studies have shown [Ratovsky et al., 2018; Ratovsky et al., 2020], statistical results for non-isolated magnetic storms are much less informative compared to those for isolated storms. For this reason, only isolated storms are used in further analysis, i.e. storms for which the time interval between neighboring events $t_0\geq$5 days. Of 556 *AE* storms, the number of isolated events is 178, i.e. ~32 %. Using the superposed epoch method with key moments corresponding to maximum *AE*, we calculated average *AE* behavior for isolated *AE* storms as a function of time relative to maximum

AE, hereinafter referred to as the reference *AE* storm. The average behavior of *Dst* was calculated in a similar way. The calculation results are presented in Figure 1.

To study the seasonal dependence of ionospheric responses, isolated *AE* storms were divided by seasons. In this case, the seasons are ~91 day intervals centered relative to solstices and equinoxes in the Northern Hemisphere: winter (November 07–December 22–February 05, 38 *AE* storms); spring (February 06–March 22–May 07, 57 *AE* storms); summer (May 08–June 22–August 07, 48 *AE* storms), and autumn (August 08–September 22–November 06, 35 *AE* storms). The dates indicate the beginning, middle, and end of the season. As will be shown in the next section, the average *AE* behaviors for different seasons differ slightly, which facilitates the interpretation of ionospheric responses, thereby allowing us to ignore the potentially different intensity of *AE* storms in different seasons.

Regional electron contents *REC*, which are weighted means of *TEC* for the selected latitude and longitude region, were utilized as ionospheric characteristics. The *TEC* values were obtained from global ionospheric maps GIM of the CODE laboratory [Schaer et al., 1998; ftp://ftp.unibe.ch/aiub/CODE/]. To calculate *REC*, we have selected five latitudinal zones in the corrected geomagnetic coordinate system: mid-latitude zones in both hemispheres 30°–60°, high-latitude zones in both hemispheres 60°–90°, and the equatorial zone ±30°. The relative (percentage) deviation of the observed values from the 27-day running mean of *REC* was employed to calculate *REC* disturbances (Δ*REC*). Using the superposed epoch method with key moments corresponding to maximum *AE*, we calculated the average behavior of Δ*REC* as a function of time relative to maximum *AE* (reference ionospheric response) for isolated winter, spring, summer, and autumn *AE* storms.

ANALYSIS OF REFERENCE IONOSPHERIC RESPONSES TO ISOLATED MAGNETIC STORMS

Figure 2 illustrates the average behavior of *AE* for four seasons and reference ionospheric responses for four seasons and five latitudinal zones. In all cases, the season refers to winter, spring, autumn, and summer in the Northern Hemisphere.

The average behavior of AE is demonstrated to vary slightly for different seasons. This means that the average intensity of AE storms is approximately the same in different seasons, which, in turn, facilitates the analysis of seasonal differences in ionospheric responses. The analysis

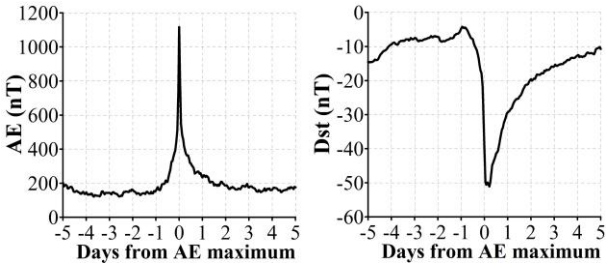

Figure 1. Average behavior of *AE* (*a*) and *Dst* (*b*) as a function of time (in days) relative to maximum *AE*

analysis shows that according to the behavior during the storm main and early recovery phases all responses can be divided into three types: type A, type N, and type V. Type A responses are predominantly positive disturbances and are observed for all seasons at equatorial latitudes and for local winters at midlatitudes of both hemispheres. A positive peak of the response is recorded 3–4 hrs after maximum *AE*, i.e. near the beginning of the recovery phase. Type N responses are disturbances with well-defined positive and negative phases, and occur at midlatitudes in spring, autumn, and local summer, and at high latitudes in spring, autumn, and local winter. A positive peak of the response is observed 2–3 hrs after maximum *AE* in the mid-latitude zone and 1–2 hrs after maximum *AE* in the high-latitude zone, i.e., as in the equatorial zone, near the beginning of the recovery phase. The time of a negative peak of the response exhibits significant seasonal variations. In spring and local summer at midlatitudes, as well as in spring and autumn at high latitudes, the peaks are detected 15–19 hrs after maximum *AE*. In autumn at midlatitudes and in local winter at high latitudes of the Northern Hemisphere, the peaks are observed 33–35 hrs after maximum *AE*. The intermediate position corresponds to the peak occurring 22 hrs after maximum *AE*, which is recorded in local winter at high latitudes of the Southern Hemisphere. Type V responses are predominantly negative disturbances and are observed for local summers at high latitudes. A negative peak of the response occurs 7–15 hrs after maximum *AE*.

Table 1 lists maximum and minimum values of *AE* and reference ionospheric responses Δ*REC*. Maximum positive disturbances of *REC* (if there are any) are seen to occur first at high latitudes (1 hr after maximum *AE*), eventually moving through midlatitudes to the equator.

The seasonal behavior of ionospheric responses can be considered in terms of the local winter—equinoxes—local summer concept, which suggests that extreme response values (positive and negative) take place in local winter or summer with intermediate values at equinoxes. Responses in the Southern Hemisphere for the midlatitude and high-latitude zones fully fit into this concept: the amplitude of the positive response increases sequentially from local summer to local winter, the amplitude of the negative response decreases sequentially from local summer to local winter. The concept also includes positive responses in the equatorial zone: the amplitude of the positive response increases sequentially from local summer to local winter in the Southern Hemisphere. There are a number of exceptions in the Northern Hemisphere. At midlatitudes, the amplitude of the positive response increases according to the spring—summer—autumn—winter pattern, and the amplitudes of the negative responses are close to each other with the highest amplitude in autumn and the lowest one in spring. At high latitudes, the amplitude of the positive response fits into the concept, and the amplitude of the negative response decreases according to the autumn—summer—winter—spring pattern.

Figure 2 shows that significant ionospheric responses occur during the pre-storm phase (from the beginning of

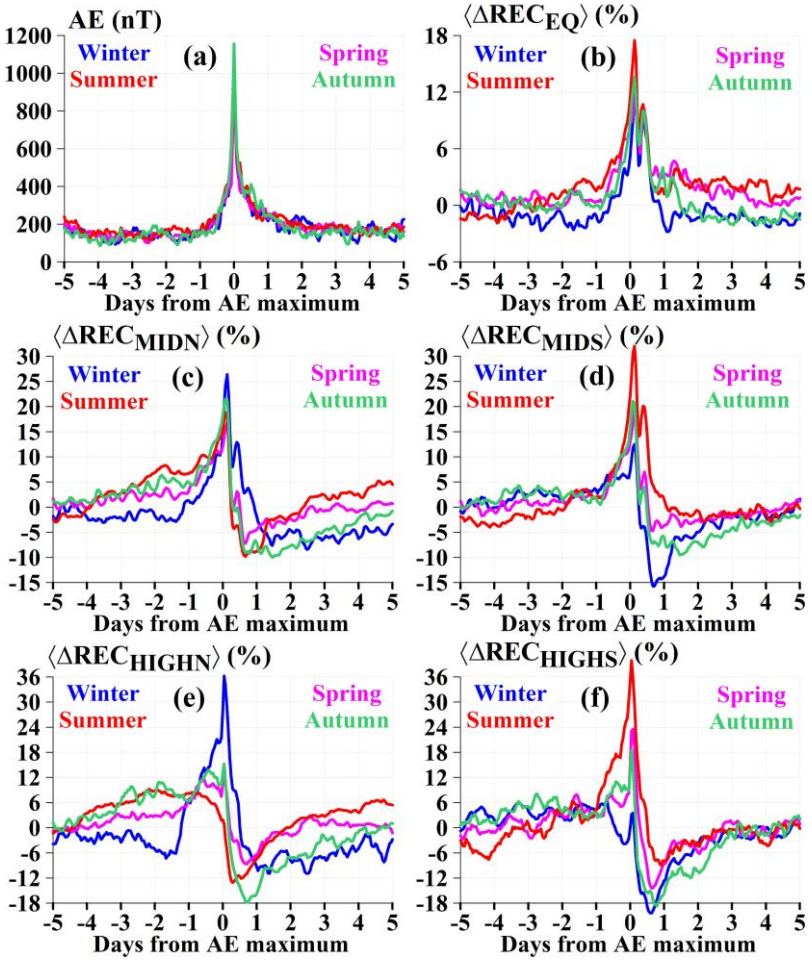

Figure 2. Average *AE* (*a*) and reference ionospheric responses for the equatorial zone (*b*), the mid-latitude zone of the Northern (*c*) and Southern (*d*) hemispheres, and the high-latitude zone of the Northern (*e*) and Southern (*f*) hemispheres. By a season is meant winter, spring, autumn, and summer in the Northern Hemisphere

Table 1

Maximum (max.) and minimum (min.) values of *AE*
and reference ionospheric responses Δ*REC*

AE, nT					Δ*REC*, equatorial zone, %				
season	max	hours	min	hours	season	max	hours	min	hours
winter (A)	1144	0	*92*	*–40*	winter (A)	11.1	3	*–2.8*	*26*
spring (A)	1066	0	*100*	*–61*	spring (A)	12.9	4	*–0.4*	*–51*
autumn (A)	1156	0	*86*	*–95*	autumn (A)	13.6	3	*–2.1*	*73*
summer (A)	1129	0	*116*	*–61*	summer (A)	17.5	3	*–1.9*	*–94*
Δ*REC*, mid-latitude zone of the Northern Hemisphere					Δ*REC*, mid-latitude zone of the Southern Hemisphere				
season	max	hours	min	hours	season	max	hours	min	hours
winter (A)	26.4	3	*–8.4*	*60*	winter (N)	12.5	3	–15.7	16
spring (N)	16.7	3	–7.2	15	spring (N)	19.4	3	–4.7	16
autumn (N)	21.5	2	–10	35	autumn (N)	21.1	2	–9.5	35
summer (N)	18.8	2	–9.8	16	summer(A)	32	3	*–4*	*-99*
Δ*REC*, high-latitude zone of the Northern Hemisphere					Δ*REC*, high-latitude zone of the Southern Hemisphere				
season	max	hours	min	hours	season	max	hours	min	hours
winter (N)	36.2	1	–10.9	33	winter (V)	*6.2*	*–17*	–20.4	15
spring (N)	13	1	–8.7	17	spring (N)	23.5	2	–14.4	15
autumn (N)	15.2	1	–17.8	17	autumn (N)	18.6	1	–18.7	19
summer (V)	*9.2*	*-52*	–13.1	7	summer (N)	39.9	1	–9	22

By a season is meant winter, spring, autumn, and summer in the Northern Hemisphere. The sign after the season indicates the response type; hours are the observation time of max. and min. relative to maximum *AE*. Slightly pronounced extremes are marked in italics.

day –5 to the beginning of day –1). The greatest positive responses are seen in summer (+8÷+9 %) and autumn (+6÷+11 %) in the mid- and high-latitude zones of the Northern Hemisphere. In the Southern Hemisphere, the positive response is less pronounced and does not have a distinct seasonal pattern. The greatest negative responses are observed in the local winter in the mid- and high-latitude zones of both hemispheres (–3÷–4 % in the mid-latitude zone and –7÷–8 % in the high-latitude zone). Of four days of the pre-storm phase, day –2 stands out, when the most positive and most negative responses are recorded in the Northern Hemisphere. In the Southern Hemisphere, day –2 is not prominent.

Figure 2 allows us to estimate after-storm effects by analyzing the response behavior during the storm late recovery phase (from the beginning of day 2 to the end of day 4). In the Southern Hemisphere during the late recovery phase, all responses reach approximately zero levels, demonstrating the absence of an after-storm effect. The autumn and spring responses in the Northern Hemisphere display similar behavior. The summer response in the Northern Hemisphere shifts from negative to positive phase during the late recovery phase, which means the classic after-storm effect described in [Ratovsky et al., 2018]. The winter response in the Northern Hemisphere during the storm late recovery phase varies about a negative level (–5 % in the mid-latitude zone and –6 % in the high-latitude zone), thereby exhibiting a negative after-storm effect.

DISCUSSION AND INTERPRETATION OF REFERENCE IONOSPHERIC RESPONSES TO ISOLATED MAGNETIC STORMS

A modification of the statistical approach to studying ionospheric responses to geomagnetic storms, based on the use of hourly resolution instead of daily resolution and *AE* instead of *Dst*, has allowed us to obtain the following advantages compared to the previously developed method [Ratovsky et al., 2020]. Previously, the time of occurrence of the greatest positive response varied within two days relative to the day corresponding to minimum *Dst*. With the new approach, this time is concentrated within 1–4 hrs after maximum *AE*. The temporary concentration of the positive response led to a significant increase in its amplitude: 18 % in the equatorial zone, 26–32 % in the mid-latitude zone, and 36–40 % in the high-latitude zone; previously, they were 8 %, 14–18 %, and 12–18 %. The seasonal pattern in the equatorial zone has become clearer: for unexplained reasons, the spring response used to be ~1.5 times higher than the responses in other seasons, now the response fits into the winter—equinoxes—summer concept. The pattern of the after-storm effect has been simplified: now the effect is reduced to a positive after-storm effect in summer and a negative after-storm effect in winter for responses in the Northern Hemisphere.

The thermospheric storm concept [Mayr et al., 1978; Brjunelli, Namgaladze, 1988; Field, Rishbeth, 1997; Buonsanto, 1999; Mikhailov, 2000; Mendillo, 2006; Prölss, 2008; Ratovsky et al., 2018] suggests that the changes in thermospheric neutral composition and neutral wind caused by heating in the high-latitude zone are the main factors determining the ionospheric response to a geomagnetic storm. Within this concept, negative disturbances of the electron density N_e in the high-latitude zone are expected due to a negative disturbance of the atomic oxygen to molecular nitrogen ratio $n(O)/n(N_2)$. Positive disturbances of N_e are expected in the equatorial zone due to a positive disturbance of $n(O)/n(N_2)$. In the mid-latitude zone, N_e disturbances can be both positive and negative, and if there are disturbances of both types the positive disturbance should precede the negative one. In the mid-latitude zone, the following seasonal dependence of N_e disturbances is expected: the strongest negative disturbances in local summer and the greatest positive ones in local winter with intermediate disturbances during equinoxes.

The analysis of reference ionospheric responses to isolated magnetic storms carried out in the previous section shows that positive responses in the equatorial zone and the seasonal pattern of the responses in the mid-latitude zone of the Southern Hemisphere fully fit into the thermospheric storm concept. There are a number of exceptions to the seasonal behavior of responses in the mid-latitude zone of the Northern Hemisphere, which were noted in the previous section as exceptions to the local winter—equinoxes—local summer concept. The thermospheric storm concept does not include positive responses of *REC* in the high-latitude zone (the largest among all latitudinal zones). The similarity between seasonal response patterns in the mid-latitude and high-latitude zones of the Southern Hemisphere seems inexplicable.

The responses of the high-latitude zone show the need to take into account the mechanisms of formation of positive disturbances, which are absent in the thermospheric storm concept. Changes in N_e within this pattern primarily relate to heights near the F2-layer maximum. As the height increases, the effect of changes in the thermospheric neutral composition weakens, and the electron temperature effect increases. An increase in the electron temperature leads to an increase in the topside scale height (depth), which can eventually cause a positive disturbance of *TEC* (which is proportional to the topside scale height) during a negative disturbance of N_e near the F2-layer maximum. This version is confirmed by the results obtained in [Astafyeva et al., 2015; Lei et al., 2015; Liu et al., 2016; Klimenko et al., 2017], where it has been shown that the responses of the bottomside and topside ionospheres to a geomagnetic storm may have the opposite sign. The similarity between the seasonal response patterns in the mid-latitude and high-latitude zones of the Southern Hemisphere can be explained as follows. In winter conditions, the topside background scale height is minimum relative to other seasons, and hence the effect of increasing scale height leads to the greatest positive disturbance of *TEC*. In summer conditions, the topside background scale height is maximum, and the effect of increasing the scale height

causes the least positive disturbance of *TEC*. As a result, the local winter—equinoxes—local summer concept is realized.

Comparing the responses in the Northern and Southern hemispheres, the following manifestations of hemispheric asymmetry can be identified. During the storm early recovery phase, the response is more pronounced in the Southern Hemisphere for the mid-latitude and high-latitude zones: the amplitude of both positive and negative responses is higher in the Southern Hemisphere than in the Northern Hemisphere. Responses in the Southern Hemisphere fully fit into the local winter—equinoxes—local summer concept, whereas in the Northern Hemisphere there are a number of exceptions. During the pre-storm phase in the Southern Hemisphere, the positive response is less pronounced and does not have a distinct seasonal pattern. There is no after-storm effect in the Southern Hemisphere during the late recovery phase. The interhemispheric asymmetry of mid-latitude ionospheric responses to geomagnetic storms was also found by the previously developed method [Ratovsky et al., 2020]. Two versions explaining the interhemispheric asymmetry have been discussed in [Ratovsky et al., 2020]: (1) the interhemispheric asymmetry of the thermospheric background neutral composition [Titheridge and Buonsanto, 1988] and (2) the responses of N_e and thermospheric density are more sensitive to geomagnetic storms in the Southern Hemisphere than in the Northern Hemisphere [Ercha et al., 2012]. An important addition to the work [Ratovsky et al., 2020] is that in this study the interhemispheric asymmetry was found not only in the mid-latitude zone, but also in the high-latitude zone. In our opinion, this addition is an argument for version (2) since version (1) provided an interpretation for the mid-latitude zone, whereas version (2) dealt with the response in all latitudinal zones. Note that this version does not explain the interhemispheric asymmetry in the pre-storm and late recovery phases.

In the previous study, ionospheric responses in the pre-storm phase were characterized as a monotonous increase in average Δ*REC*. In this study, of four days of the pre-storm phase day –2 stands out when in the Northern Hemisphere there are the greatest positive (in summer and autumn) and greatest negative (in winter) responses, whereas in the Southern Hemisphere day –2 is not prominent. Day –2 does not reveal itself at all in average *AE* either (see Figure 2). This makes it possible, following Burešova, Laštovička [2007], to exclude auroral activity expressed through *AE* as the cause of positive response. The revealed seasonal dependence (the most positive response in summer and autumn) is partially consistent with the results obtained in [Burešova, Laštovička 2007], where an increased intensity of pre-storm positive disturbances of N_mF2 was observed in summer. Both seasonal dependence and interhemispheric asymmetry allow us to exclude any manifestation of solar activity as a cause for a positive response. The revealed interhemispheric asymmetry of the response behavior in the pre-storm phase adds ambiguity to the explanation of ionospheric disturbances during the pre-storm phase.

ANALYSIS OF DIFFERENCES IN THE IONOSPHERIC RESPONSE ON EVENTS, IDENTIFIED BY THE *Dst* AND *AE* INDICES

It is interesting to analyze the differences in the ionospheric response to geomagnetic events identified by *Dst* and *AE*. The criterion for a geomagnetic event identified by *Dst* was the fulfillment of two conditions: 1) $Dst(t_0)$ is the lowest *Dst* on the time interval $t_0 \pm 12$ hrs; 2) $Dst(t_0) \leq -50$ nT, where t_0 is the time corresponding to minimum *Dst*. According to [Gonzalez et al., 1994; 1999], events identified by *Dst* are geomagnetic storms in the classical sense. The events identified by the indices are designated as *AE* and *Dst* storms.

Dst storms can be divided into three groups (Table 2). The first consists of isolated *Dst* storms, which are simultaneously isolated *AE* storms; the second includes isolated *Dst* storms, which are non-isolated *AE* storms. The third group contains isolated *Dst* storms, which are not *AE* storms (the *AE* value is below the *AE* storm threshold).

Assuming that the ionospheric response is more closely related to *AE* than to *Dst*, the following differences can be expected. Storms of the first group do not make any difference in responses. Responses to *Dst* storms of the second group are expected to be more negative since ionospheric disturbances occur against the negative phase of responses to the previous *AE* storm (or storms). Responses to *Dst* storms of the third group are expected to be less pronounced (a decrease in the amplitudes of both positive and negative responses) due to lower *AE* during these *Dst* storms. Note that when averaged the effect of storms of the second group (an increase in negative response) competes with the effect of storms of the third group (a decrease in negative response).

The greatest difference between the responses to *AE* and *Dst* storms was obtained for the high-latitude zone of the Southern Hemisphere (Figure 3). It is apparent that the responses to summer *Dst* storms are more negative (a decrease in the amplitude of the positive response and an increase in the amplitude of the negative response), while the responses to winter, spring, and autumn *Dst* storms are less pronounced (a decrease in the amplitudes of both positive and negative responses). This seasonal difference is explained by the fact that (see Table 2) the contribution of *Dst* storms, which are non-isolated *AE* storms, is maximum for the summer season (32 %), whereas for other seasons this contribution is much smaller (9 % for winter and 15 % for spring and autumn). For winter, spring, and autumn, the contribution of *Dst* storms, which are not *AE* storms, dominates (*AE* is below the *AE* storm threshold). Thus, the difference between the responses to *AE* and *Dst* storms for the high-latitude zone of the Southern Hemisphere accords with the assumption that the ionospheric response is more closely related to *AE* than to *Dst*.

A common property of the difference between the responses to *AE* and *Dst* storms for all latitudinal zones is that the responses to summer *Dst* storms are more negative. Yet, the fact that the responses to spring and autumn *Dst*

Table 2

AE storms of various types included into the list of isolated *Dst* storms for different seasons

Type of *AE* storm/Season	Winter	Spring	Summer	Autumn
Isolated *AE* storms	50 %	46 %	55 %	48 %
Non-isolated *AE* storms	9 %	15 %	32 %	15 %
Events that are not *AE* storms	41 %	39 %	13 %	37 %

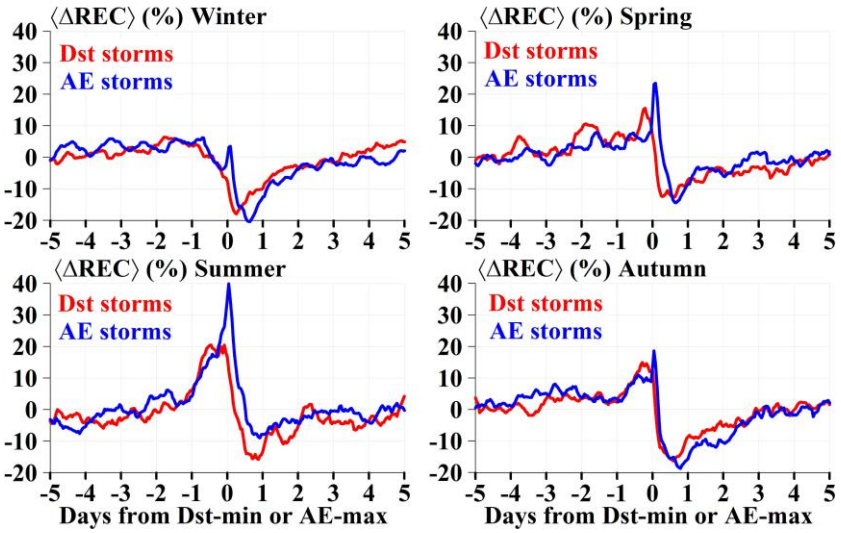

Figure 3. High-latitude zone of the Southern Hemisphere. Ionospheric responses to *Dst* storms as a function of time relative to minimum *Dst* (red curves) and to *AE* storms as a function of time relative to maximum *AE* (blue curves)

storms are less pronounced is observed only for the high-latitude zone of the Southern Hemisphere (for other zones, the responses are similar). The responses to winter *Dst* storms are also less pronounced for the high-latitude zone of the Northern Hemisphere and the mid-latitude zone of the Southern Hemisphere (for the mid-latitude zone of the Northern Hemisphere and the equatorial zone, the responses are similar). This latitudinal difference in the comparison of responses to *AE* and *Dst* storms currently has no explanation and requires further research.

CONCLUSION

The statistical study of responses of the regional electron content to geomagnetic events at high, middle, and equatorial latitudes by the superposed epoch method using the *AE* index has allowed us to obtain the following main results.

Regional electron content responses can be divided into three types: type A (predominantly positive disturbance), type N (disturbance having distinct positive and negative phases) and type V (predominantly negative disturbance). Positive peaks are largely recorded within 1–4 hrs after maximum *AE*. Negative peaks have a wide range from 7 to 35 hrs after maximum *AE*.

Positive responses in the equatorial zone and the seasonal pattern of responses in the mid-latitude zone of the Southern Hemisphere fully correspond to the thermospheric storm concept. There are a number of exceptions to the seasonal behavior of responses in the mid-latitude zone of the Northern Hemisphere. Positive responses in the high-latitude zone do not fit into the thermospheric storm concept.

An increase in the electron temperature, which leads to an increase in the topside scale height and a corresponding increase in the total electron content, is proposed as the cause for the positive responses in the high-latitude zone. The greatest effect is observed under winter conditions when the topside background scale height is minimum relative to other seasons.

Interhemispheric asymmetry of responses reveals itself in all geomagnetic storm phases. In the storm early recovery phase, the amplitude of both positive and negative responses is higher in the Southern Hemisphere than in the Northern Hemisphere. During the pre-storm phase in the Southern Hemisphere, the positive response is less pronounced and does not have a distinct seasonal pattern. There is no after-storm effect in the Southern Hemisphere during the late recovery phase. To explain the interhemispheric asymmetry of the responses, a version is proposed that the responses of electron and thermospheric densities are more sensitive to geomagnetic storms in the Southern Hemisphere than in the Northern Hemisphere. The interhemispheric asymmetry during the pre-storm and late recovery phases currently has no explanation, even in the form of versions.

The main factor influencing the difference between ionospheric responses to *AE* and *Dst* storms is that some isolated *Dst* storms are non-isolated *AE* storms. The influence of this factor depends on the percentage contribution of non-isolated *AE* storms to isolated *Dst* storms. The maximum contribution (32 %) takes place for the summer season, which leads to the fact that for

all latitudinal zones responses to summer *Dst* storms are more negative than responses to summer *AE* storms.

The research was financially supported by the Russian Science Foundation (Grant No. 23-27-00213). OMNI data was obtained through the GSFC/SPDFOMNI-Web interface on the website [https://omniweb.gsfc.nasa.gov].

We thank the CODE laboratory for the global ionospheric maps available at [ftp://ftp.unibe.ch/aiub/CODE/]. The primary data sets on regional electron content were obtained using the SIMuRG system, website [https://simurg.iszf.irk.ru/].

REFERENCES

Araujo-Pradere E.A., Fuller-Rowell T.J., Codrescu M.V., Bilitza D. Characteristics of the ionospheric variability as a function of season latitude local time and geomagnetic activity. *Radio Sci*. 2005, vol. 40, RS5009. DOI: 10.1029/2004 RS003179.

Astafyeva E., Zakharenkova I., Förster M. Ionospheric response to the 2015 St. Patrick's Day storm: A global multi-instrument overview. *J. Geophys. Res.: Space Phys*. 2015, vol. 120, no. 10, pp. 9023–9037. DOI: 10.1002/2015 JA021629.

Brjunelli B.E., Namgaladze A.A. Fizika ionosfery [Physics of the ionosphere]. Moscow, Nauka, 1988, 528 p. (In Russian).

Buonsanto M.J. Ionospheric Storms: A Review. *Space Sci. Rev*. 1999, vol. 88, no. 3-4, pp. 563–601. DOI: 10.1023/ A:1005107532631.

Burešová D., Laštovička J. Pre-storm enhancements of f_oF2 above Europe. *Adv. Space Res*. 2007, vol. 39, no. 8, pp. 1298–1303. DOI: 10.1016/j.asr.2007.03.003.

da Silva R.P., Denardini C.M., Marques M.S., Resende L.C.A., Moro J., et al. Ionospheric total electron content responses to HILDCAA intervals. *Ann. Geophys*. 2020, vol. 38, no. 1, pp. 27–34. DOI: 10.5194/angeo-38-27-2020.

Deminov M.G., Deminova G.F., Zherebtsov G.A., Polekh N.M. Statistical properties of variability of the quiet ionosphere F2-layer maximum parameters over Irkutsk under low solar activity. *Adv. Space Res*. 2011, vol. 51, no. 5, pp. 702–711. DOI: 10.1016/j.asr.2012.09.037.

Ercha A., Ridley A.J., Zhang D., Xiao Z. Analyzing the hemispheric asymmetry in the thermospheric density response to geomagnetic storms. *J. Geophys. Res*. 2012, vol. 117, no. A08317. DOI: 10.1029/2011JA017259.

Field P.R., Rishbeth H. The response of the ionospheric F2-layer to geomagnetic activity: an analysis of wordwide data. *J. Atmos. Terr. Phys*. 1997, vol. 59, no. 2, pp. 163–180. DOI: 10.1016/S1364-6826(96)00085-5.

Gonzalez W.D., Joselyn J.A., Kamide Y., Kroehl H.W., Rostoker G., Tsurutani B.T., et al. What is a geomagnetic storm? *J. Geophys. Res*. 1994, vol. 99, no. A4, pp. 5771–5792. DOI: 10.1029/93JA02867.

Gonzalez W.D., Tsurutani B.T., Clúa de Gonzalez A.L. Interplanetary origin of geomagnetic storms. *Space Sci. Rev*. 1999, vol. 88, pp. 529–562. DOI: 10.1023/A:1005160129098.

Klimenko M.V., Klimenko V.V., Ratovsky K.G., Goncharenko L.P., Sahai Y., Fagundes P.R., et al. Numerical modeling of ionospheric effects in the middle- and low-latitude F region during geomagnetic storm sequence of 9–14 September 2005. *Radio Sci*. 2011, vol. 46, no. 3, RS0D03. DOI: 10.1029/2010RS004590.

Klimenko M.V., Klimenko V.V., Zakharenkova I.E., Ratovsky K.G., Korenkova N.A., Yasyukevich Yu.V., et al. Similarity and differences in morphology and mechanisms of the f_oF2 and *TEC* disturbances during the geomagnetic storms on 26–30 September 2011. *Ann. Geophys*. 2017, vol. 35, no. 4, pp. 923–938. DOI: 10.5194/angeo-35-923-2017.

Klimenko M.V., Klimenko V.V., Sukhodolov T.V., Bessarab F.S., Ratovsky K.G., Rozanov E.V. Role of internal atmospheric variability in the estimation of ionospheric response to solar and magnetospheric proton precipitation in January 2005. *Adv. Space Res*. 2023, vol. 71, iss. 11, pp. 4576–4586. DOI: 10.1016/j.asr.2023.01.012.

Lei J., Zhu Q., Wang W., Burns A.G., Zhao B., Luan X., Zhong J., Dou X.. Response of the topside and bottomside ionosphere at low and middle latitudes to the October 2003 superstorms. *J. Geophys. Res.: Space Phys*. 2015, vol. 120, no. 8, pp. 6974–6986. DOI: 10.1002/2015JA021310.

Liu J., Wang W., Burns A., Yue X., Zhang S., Zhang Y., Huang C. Profiles of ionospheric storm-enhanced density during the 17 March 2015 great storm. *J. Geophys. Res.: Space Phys*. 2016, vol. 121, no. 1, pp. 727–744. DOI: 10.1002/ 2015JA021832.

Lu G., Richmond A.D., Roble R.G., Emery B.A. Coexistence of ionospheric positive and negative storm phases under northern winter conditions: A case study *J. Geophys. Res*. 2001, vol. 106, no. A11, pp. 24493–24504. DOI: 10.1029/ 2001JA000003.

Marques de Souza Franco A., Hajra R., Echer E., Bolzan M.J.A. Seasonal features of geomagnetic activity: a study on the solar activity dependence. *Ann. Geophys*. 2021, vol. 39, no. 5, pp. 929–943. DOI: 10.5194/angeo-39-929-2021.

Mayr H.G., Harris I., Spencer N.W. Some properties of upper atmosphere dynamics. *Rev. Geophys. Space Phys*. 1978, vol. 16, pp. 539–565. DOI: 10.1029/RG016i004p00539.

Mendillo M. Storms in the ionosphere: Patterns and processes for total electron content. *Rev. Geophys*. 2006, vol. 44, RG4001. DOI: 10.1029/2005RG000193.

Mikhailov A.V. Ionospheric F2-layer storms. *Fis. Tierra*. 2000, vol. 12, pp. 223–262.

Pedatella N.M. Impact of the lower atmosphere on the ionosphere response to a geomagnetic superstorm. *Geophys. Res. Lett*. 2016, vol. 43, pp. 9383–9389. DOI: 10.1002/2016GL070592.

Pedatella N.M., Liu H.-L. The influence of internal atmospheric variability on the ionosphere response to a geomagnetic storm. *Geophys. Res. Lett*. 2018, vol. 45, no. 10, pp. 4578–4585. DOI: 10.1029/2018GL077867.

Prölss G.W. Ionospheric F-region storms: unsolved problems. *Characterizing the Ionosphere. Meeting Proc. RTO-MP739 IST-056*. Paper 10. Neuilly-sur-Seine, France: RTO. 2006, pp. 10-1–10-20.

Prölss G.W. Ionospheric storms at mid-latitudes: A short review. *Midlatitude Ionospheric Dynamics and Disturbances, AGU Monograph*. 2008, vol. 181, pp. 9–24.

Ratovsky K.G., Klimenko M.V., Klimenko V.V., Chirik N.V., Korenkova N.A., Kotova D.S. After-effects of geomagnetic storms: Statistical analysis and theoretical explanation. *Solar-Terrestrial Physics*. 2018, vol. 4, no. 4, pp. 26–32. DOI: 10.12737/stp-44201804.

Ratovsky K.G., Klimenko M.V., Yasyukevich Yu.V., Klimenko V.V., Vesnin A.M. Statistical analysis and interpretation of high-, mid- and low-latitude responses in regional electron content to geomagnetic storms. *Atmosphere*. 2020, vol. 11, no. 12, p. 1308. DOI: 10.3390/atmos11121308.

Ratovsky K.G., Klimenko M.V., Vesnin A.M., Belyuchenko K.V., Yasyukevich Yu.V. Comparative analysis of geomagnetic events identified according to different indices. *Bull.*

Russ. Acad. Sci. Phys. 2024, vol. 88, no. 3, pp. 296–302. DOI: 10.1134/S1062873823705433.

Rishbeth H., Mendillo M. Patterns of F2-layer variability. *J. Atmos. Solar-Terr. Phys*. 2001, vol. 63, pp. 1661–1680. DOI: 10.1016/S1364-6826(01)00036-0.

Rodger A.S., Wrenn G.L., Rishbeth H. Geomagnetic storms in the Antarctic F-region. II. Physical interpretation. *J. Atmos. Terr. Phys*. 1989, vol. 51, no. 11-12, pp. 851–866. DOI: 10.1016/0021-9169(89)90002-0.

Schaer S., Beutler G., Rothacher M. Mapping and predicting the ionosphere. *Proc. IGS AC Workshop*. Darmstadt, Germany, 1998, pp. 307–320.

Titheridge J.E., Buonsanto M.J. A Comparison of Northern and Southern hemisphere TEC storm behavior. *J. Atmos. Terr. Phys*. 1988, vol. 50, no. 9, pp. 763–780. DOI: 10.1016/0021-9169(88)90100-6.

Wrenn G.L., Rodger A.S., Rishbeth H. Geomagnetic storms in the Antarctic F-region. I. Diurnal and seasonal patterns for main phase effects. *J. Atmos. Terr. Phys*. 1987, vol. 49, no. 9, pp. 901–913. DOI: 10.1016/0021-9169(87)90004-3.

URL: https://omniweb.gsfc.nasa.gov (accessed May 6, 2023).

URL: ftp://ftp.unibe.ch/aiub/CODE/ (accessed December 1, 2023).

URL: https://simurg.iszf.irk.ru/ (accessed December 1, 2023).

Original Russian version: Ratovsky K.G., Klimenko M.V., Vesnin A.M., Belyuchenko K.V., published in Solnechno-zemnaya fizika. 2025, vol. 11, no. 2, pp. 79–88. DOI: 10.12737/szf-112202507.

How to cite this article

Ratovsky K.G., Klimenko M.V., Vesnin A.M., Belyuchenko K.V. Regional electron content responses to geomagnetic events at high, middle, and equatorial latitudes obtained by superposed epoch method using *AE* index. *Sol.-Terr. Phys.* 2025, vol. 11, iss. 2, pp. 69–77. DOI: 10.12737/stp-112202507.